Published in final edited form as:
Drug Deliv Transl Res. 2013 June 1; 3(3): 260–271. doi:10.1007/s13346-012-0119-6.

COMPARATIVE PHARMACOKINETICS OF PAMAM-OH DENDRIMERS AND HPMA COPOLYMERS IN OVARIAN-TUMOR-BEARING MICE

S. Sadekar[a,b,#], **O. Linares**[c,#], **GJ. Noh**[g], **D. Hubbard**[b,d], **A. Ray**[a,b], **M. Janát-Amsbury**[a,b,e], **C. M. Peterson**[a,b,e], **J. Facelli**[b,c,f,*], and **H. Ghandehari**[a,b,d,*]

[a]Department of Pharmaceutics and Pharmaceutical Chemistry, University of Utah, Salt Lake City, Utah, 84108, USA

[b]Center for Nanomedicine, Nano Institute of Utah, University of Utah, Salt Lake City, Utah, 84108, USA

[c]Biomedical Informatics, University of Utah, Salt Lake City, Utah, 84108, USA

[d]Department of Bioengineering, University of Utah, Salt Lake City, Utah, 84108, USA

[e]Department of Obstetrics and Gynecology, University of Utah, Salt Lake City, Utah, 84108, USA

[f]Center for High Performance Computing, University of Utah, Salt Lake City, Utah, 84108, USA

[g]Department of Clinical Pharmacology and Therapeutics/Anesthesiology and Pain Medicine Asan Medical Center, University of Ulsan College of Medicine, Republic of Korea

Abstract

The purpose of this study was to model data from a head to head comparison of the *in vivo* fate of hyper-branched PAMAM dendrimers with linear HPMA copolymers in order to understand the influence of molecular weight (MW), hydrodynamic size (Rh) and polymer architecture on biodistribution in tumor-bearing mice using compartmental pharmacokinetic analysis. Plasma concentration data was modeled by two-compartment analysis using Winnonlin® to obtain elimination clearance (E.CL) and plasma exposure (AUC_{plasma}). Renal clearance (CL_R) was calculated from urine data collected over 1 week. A plasma-tumor link model was fitted to experimental plasma and tumor data by varying the tumor extravasation (K_4, K_6) and elimination (K_5) rate constants using multivariable constrained optimization solver in Matlab®. Tumor exposures (AUC_{tumor}) were computed from area under the tumor concentration time profile curve by the linear trapezoidal method. Along with MW and Rh, polymer architecture was critical in

[*]Corresponding authors: Hamidreza Ghandehari, PhD, Departments of Pharmaceutics & Pharmaceutical Chemistry, and Bioengineering, Utah Center for Nanomedicine, Nano Institute of Utah, University of Utah, 5215 SMBB, 36 S. Wasatch Dr., Salt Lake City, UT 84112-5001, Tel: (801) 587-1566, Fax: (801) 585-0575, hamid.ghandehari@pharm.utah.edu. Julio C. Facelli, PhD, Department of Biomedical Informatics Center for High Performance Computing, University Of Utah, 155 S 1452 E RM 405, SALT LAKE CITY UT 84112-0190, CHPC 801-585-3791, BMI 801-581-4080, Julio.Facelli@utah.edu.
[#]Authors contributed equally to the work

The authors of this manuscript have no competing interests as defined by Springer; they do not have any other interests that influence the results and discussion of this paper.

Integrity of Research and Reporting: This work was performed in compliance with the current laws of the United States of America.

Online resource describes detailed synthesis of HPMA copolymer (131 kDa) (Section I), biodistribution of HPMA copolymer (131 kDa) and biodistribution of all the polymers in non-target elimination organs kidney and liver (Section II), akaike information criterion values for plasma compartment models (Section III), renal clearance calculations (Section IV), polymer interactions with bovine serum albumin (Section V), equations describing plasma concentration time profile (Section VI) and compartmental model equations for extravasation and elimination rate constants (Section VII).

affecting the blood and tumor pharmacokinetics of the PAMAM-OH dendrimers and HPMA copolymers. Elimination clearance decreased more rapidly with increase in hydrodynamic size for PAMAM-OH dendrimers as compared to HPMA copolymers. HPMA copolymers were eliminated renally to a higher extent than PAMAM-OH dendrimers. These results are suggestive of a difference in extravasation of polymers of varying architecture through the glomerular basement membrane. While the linear HPMA copolymers can potentially reptate through a pore smaller in size than their hydrodynamic radii in a random coil conformation, PAMAM dendrimers have to deform in order to permeate across the pores. With increase in molecular weight or generation, the deforming capacity of PAMAM-OH dendrimers is known to decrease, making it harder for higher generation PAMAM-OH dendrimers to sieve through the glomerulus as compared to HPMA copolymers of comparable molecular weights. PAMAM-OH dendrimer had greater tumor extravsation rate constants and higher tumor to plasma exposure ratios than HPMA copolymers of comparable molecular weights which indicated that in the size range studied, when in circulation, PAMAM-OH dendrimers had a higher affinity to accumulate in the tumor than the HPMA copolymers.

Keywords

poly(amido amine) (PAMAM) dendrimer; *N*-(2-hydroxypropyl)methacrylamide (HPMA) copolymer; polymer architecture; compartmental pharmacokinetics

1. INTRODUCTION

Biocompatible water-soluble polymers have been widely used as carriers for a variety of drug-delivery and *in vivo* imaging applications [1]. Polymeric carriers can have varying architectures such as linear, dendritic, comb-shaped and star-shaped [2]. Poly(amido amine) or PAMAM dendrimers are a class of hyperbranched polymers which have shown promise as drug carriers for targeted delivery to solid tumors [3–5]. PAMAM dendrimers have an extraordinary level of structural control and multi-functionalizing potential. With every increase in generation of the PAMAM dendrimer, the molecular weight and number of surface groups double and their molecular conformation becomes more rigid. The pharmacokinetics of PAMAM dendrimers has been correlated to its physicochemical properties such as generation or molecular weight, chemical composition of core and nature of surface groups as well as type of surface modification [6–8].

Poly(*N*-(2-hydroxypropyl)methacrylamide) (HPMA) copolymers are a class of linear polymers with side chains that can be terminated in drugs, targeting moieties and imaging agents [9, 10]. Such copolymers have been well characterized for the influence of co-monomer structure, composition and charge on solution properties, molecular conformation as well as *in vivo* biodistribution and pharmacokinetics [11–13].

Along with the molecular weight, polymer architecture and hydrodynamic size are also known to affect the biodistribution and consequently the pharmacokinetics of the polymeric carriers [14–17]. The shape and ability of macromolecules to deform have been reported to influence their glomerular filtration and consequently elimination clearance and plasma exposure [15]. Previously in our laboratory, we have conducted a head to head comparison of the *in vivo* fate of hyper-branched hydroxyl-terminated poly(amido amine) or PAMAM-OH dendrimers with linear HPMA copolymers (containing hydroxyl-terminated side chains) of comparable molecular weights in tumor-bearing mice. It was observed that along with molecular weight, hydrodynamic size and polymer architecture were critical in affecting the accumulation of these polymers in the tumor and elimination organs such as kidney and liver [17].

To gain further insight into the biological fate of these polymers of varying architecture, it is essential to quantify the *in vivo* kinetics of these drug carriers after having obtained the tissue distribution information. The purpose of this study was to model the previously obtained experimental data on the biodistribution of HPMA copolymers and PAMAM-OH dendrimers by compartmental pharmacokinetic analysis. We also experimentally investigated an additional probe-HPMA copolymer (131 kDa), which was chemically similar to the other HPMA copolymers under study and comparable in molecular weight to PAMAM G7.0-OH. By modeling the biodistribution data, we quantified the pharmacokinetic parameters of these polymeric carriers of varying hydrodynamic sizes and architecture in order to understand their effect on *in vivo* kinetics.

2. MATERIALS AND METHODS

2.1 Data Collection

Polymer synthesis, characterization and radiolabeling—The synthesis and characterization of the polymers is described previously [17]. Briefly, HPMA copolymers containing ethanolamine side chains were synthesized to obtain weight average molecular weights of 26, 52 and 131 kDa in order to have comparable molecular weights with PAMAM dendrimers (purchased from Sigma Aldrich, MO), hydroxyl terminated, generations 5.0 (G5.0-OH-29 kDa), 6.0 (G6.0-OH-58 kDa) and 7.0 (G7.0-OH-117 kDa) respectively. Polymers were characterized using a size exclusion chromatography (SEC) system with Superose 6™ 10/300 GL column (GE Healthcare, Piscataway, NJ) to estimate molecular weight using HPMA homopolymer standards of known molecular weights. They were further characterized for hydrodynamic radius (R_h) using a Dynamic Light Scattering (DLS) detector (Helleos II) attached to the FPLC system and analyzed using Astra™ 5.3.4.13 software (Wyatt Technologies, Santa Barbara, CA). The zeta potential of polymers dispersed in distilled (DI) water at a concentration of 5.0 mg/ml was measured using a Malvern Instruments Zetasizer Nano ZS (Westborough, MA). The HPMA copolymers, containing tyrosine groups in the side chains, were reacted with $Na^{125}I$ (American Radiolabeled Chemicals, St. Louis, MO) while PAMAM dendrimers were reacted with ^{125}Iodine-labeled Bolton Hunter reagent (American Radiolabeled Chemicals, St. Louis, MO) to facilitate radioactive detection. The synthesis and characterization of all the polymers described above, with the exception of HPMA copolymer (131 kDa) was reported previously [17]. The HPMA copolymer (131 kDa) was synthesized (Detailed methodology in Section I, online resource) and characterized in order to provide a random-coil system comparable in MW to the hyperbranched PAMAM G7.0-OH.

***In vivo* Biodistribution—**The *in vivo* biodistribution of the polymers in ovarian tumor bearing mice was described previously [17]. Briefly, animals were inoculated with approximately 1×10^6 A2780 cells directly beneath the left ovarian bursa. Six groups of tumor-bearing mice were dosed intravenously by tail vein injection with 50 mg/Kg of radiolabeled G5.0-OH, HPMA copolymer (26 kDa), 40 mg/Kg of HPMA copolymer (52 kDa) and 20 mg/Kg of PAMAM G6.0-OH, G7.0-OH and HPMA copolymer (131 kDa) in 0.2 mL sterile saline. The mice were sacrificed at defined time points of 5 minute, 30 minute, 2 hour, 6 hour, 24 hour and 1 week. All major organ systems were collected including blood, heart, lung, liver, spleen, kidney, tumor, brain and the rest of the carcass that included skin, muscle and intestines. Urine and stool were collected by housing animals in metabolic cages and were pooled for all the animals for a given study group at a particular time point. Blood and homogenized carcass were sampled whereas the rest of the organs collected were measured as a whole for radioactive count using a Gamma counter (Cobra Autogamma, Perkin Elmer, Wellesley, MA). All animal experiments were performed in accordance with the University of Utah IACUC guidelines under approved protocols. More

details on the methodology of data collection is reported in the previously published biodistribution study [17]. The radioactive readings obtained in counts per minute from blood, tumor and urine were expressed as milligram of dose (weight of polymer) using the correlation of administered dose in mg/kg of mouse and total counts per minute of radioactivity measured for each dose. The blood weights of each mouse were expressed in milliliters (volume of blood) assuming the density of mouse blood to be 1.05 g/ml [18]. Consequently, the plasma concentration of polymers (C_p) was expressed as the weight of PAMAM-OH dendrimer/HPMA copolymer per unit volume of blood (mg/ml). The organ accumulation for tumor was expressed in milligram of polymer per gram of organ weight (mg/g). The biodistribution of all the polymers described above, with the exception of HPMA copolymer (131 kDa) was reported previously [17]. The biodistribution of HPMA copolymer (131 kDa) was evaluated (Figure S1–S3, Section II, online resource) in order to provide a third data point in the correlation of pharmacokinetic parameters of the HPMA copolymer series to hydrodynamic size as well as to provide a head to head comparison with pharmacokinetics of PAMAM G7.0-OH of comparable MW.

2.2 Pharmacokinetic Analysis

The biodistribution data was modeled using a naïve averaged data approach. Plasma concentration data was fitted to one and two-compartmental models with single bolus input using WinNonlin® 2.1 (Pharsight, a Certara Company, St. Louis, Missouri). The Akaike Information Criterion (AIC) values obtained from each of the model fits indicated that the two-compartment model fit the plasma concentration time profile better than the one-compartment model (Table S1, Section III, online resource). The plasma data was therefore modeled by two-compartment analysis using Winnonlin® 2.1 to obtain elimination clearance (E.CL) and plasma exposure (AUC_{plasma}). Renal clearance (CL_R) was calculated from urine data collected over 1 week (Equations (1) and (2), Section III, online resource).

A compartmental model was set up in order to link the plasma and the tumor compartments (Figure 1). The model allowed a two-compartmental distribution for the plasma between the central plasma (C_p) and the peripheral fast distribution compartment (C_f) (as determined from fitting plasma data alone). The tumor compartment was subdivided into two compartments, linked serially to the plasma. The first compartment (C_{t1}) allowed elimination of the polymers back into the plasma. The second tumor compartment (C_{t2}) did not allow elimination in order to account for the tumor retention of the higher MW polymers. The plasma elimination (K_1) and distribution (K_2, K_3) rate constants were fixed as per the two-compartmental distribution of the plasma data. The model was fitted to experimental plasma and tumor data by varying the tumor extravasation (K_4, K_6) and elimination (K_5) rate constants using multivariable constrained optimization solver in Matlab® (compartmental model equations and optimization code given in Section VII, Online Resource). The model assumed that the presence of the tumor did not alter the plasma pharmacokinetics.

Tumor exposures (AUC_{tumor}) were computed from area under the tumor concentration time profile curve by the linear trapezoidal method. Plasma and tumor exposures were dose normalized assuming linear pharmacokinetics over the dose ranges studied for the polymers (20–50 mg/Kg).

3. RESULTS

3.1. Polymer Characteristics

The detailed characteristics of the polymers employed in the study are summarized in Table I. The addition of the experimental points for high molecular weight HPMA copolymer (131 kDa), comparable in molecular weight to G7.0-OH (117 kDa), has provided more insight

into the hydrodynamic size trends as a function of molecular weight for the HPMA copolymer series. The PAMAM-OH dendrimers under study were generations 5.0, 6.0 and 7.0 with hydroxyl surface groups chosen such that their molecular weights (29, 58 and 117 kDa) lie in the physiologically relevant range for kidney filtration, extended plasma circulation and tumor retention. The HPMA copolymers (26, 52 and 131 kDa) have comparable molecular weights with PAMAM G5.0-OH, G6.0-OH and G7.0-OH dendrimers respectively. Polymer architecture affected molecular conformation and hence hydrodynamic size of the PAMAM dendrimers and HPMA copolymers of comparable molecular weights. The increment in hydrodynamic size (R_h) of HPMA copolymers with increase in molecular weight (MW) was greater than the increment in R_h of PAMAM dendrimers with the same increments in MW (Figure 2). Below a MW of about 40 kDa, PAMAM G5.0-OH (MW = 29 kDa) was larger (R_h = 2.3 nm) than HPMA copolymer of comparable MW (MW= 26 kDa, R_h = 1.4 nm). Above this cutoff of 40 kDa, the opposite trend was observed. PAMAM G6.0-OH (MW = 58 kDa, R_h = 3.0 nm) was smaller than HPMA copolymer of comparable MW (MW = 52 kDa, R_h = 3.3 nm). The trend was consistent amongst the higher MW polymers with the HPMA copolymer (MW = 131 kDa, Rh = 8.2 nm) being twice the hydrodynamic size of G7.0-OH (MW = 117 kDa, R_h = 4.0 nm) of comparable MW. The PAMAM dendrimers had hydroxyl surface groups while the HPMA copolymers had hydroxyl-terminating side chains to provide a fairly neutral charge for both the polymers of varying architecture. However, HPMA copolymers of 26 and 131 kDa had a slightly negative charge due to a hydrolysis side reaction, resulting in pendent carboxylic acid groups. This side reaction can occur in the final aminolysis step in the copolymer synthesis reaction that imparts a majority of hydroxyl-terminated surface groups.

3.2. Pharmacokinetic Analysis

The polymers showed a biphasic exponential blood circulation with an apparent fast distribution component and a much slower elimination component (Figure 3A). The two-compartmental pharmacokinetic parameter estimates showed a significant difference across molecular weights for each of the polymer series-PAMAM-OH dendrimers and HPMA copolymers (Table 2). Details of the results are discussed below:

3.2.1. Plasma Exposure—The dose normalized plasma exposure (AUC_{plasma}/dose) increased with increase in molecular weight or hydrodynamic size for the PAMAM-OH dendrimers (Table 2, Figure 3B). The HPMA copolymers had similar plasma exposures for the 26 and 52 kDa copolymers, while the plasma exposure increased drastically for the HPMA copolymer (131 kDa) (Table 2, Figure 3B). Consistent with the trend for elimination clearance (Section 3.2.2), HPMA copolymer (26 kDa) (R_h = 1.4 nm) had a higher plasma exposure in spite of being smaller in hydrodynamic size than G5.0-OH (R_h = 2.3 nm) of comparable MW. The opposite was seen for HPMA copolymer (52 kDa) (R_h = 3.3 nm) and G6.0-OH (R_h = 3.0 nm) of comparable MW with the hyperbranched dendrimer showing higher plasma exposure than HPMA copolymer of comparable MW even though the dendrimer was slightly smaller than the HPMA copolymer. This observation can also be attributed to the trend in elimination clearance where the linear HPMA copolymer on the threshold of kidney filtration eliminated faster than the branched dendrimer (elaborated in Section 3.2.2). Owing to its hydrodynamic size being twice that of G7.0-OH (R_h = 4.0 nm), HPMA copolymer (131 kDa) (R_h = 8.2 nm) had a much higher plasma exposure than G7.0-OH of comparable MW.

3.2.2. Elimination clearance-correlation with hydrodynamic size—Elimination clearance decreased with increase in molecular weight within each of the polymer series (Table 2). The hydrodynamic diameter of G5.0-OH (29 kDa) and HPMA (26 kDa) were below the threshold diameter for kidney filtration (6.0 nm) [19]. In spite of being greater in

hydrodynamic size, the plasma elimination clearance of G5.0-OH (R_h = 2.3 nm) was significantly higher than that of HPMA (26 kDa) (R_h = 1.4 nm) of comparable molecular weight. In this size range, the highly compact structure of the PAMAM dendrimer may facilitate extravasation faster than the linear HPMA copolymer, explaining its faster rate of disappearance from the plasma compartment. These observations demonstrate that polymer architecture affected elimination clearance below kidney filtration threshold. G6.0-OH (58 kDa) and HPMA copolymer (52 kDa) were on the threshold of kidney filtration cutoff diameter (6.0 nm). Their elimination clearances were comparable with the HPMA (R_h = 3.3 nm) being eliminated from the plasma slightly faster than the G6.0-OH (R_h = 3.0 nm). This difference was not statistically significant. However this observation suggests that at the kidney filtration threshold size, the linear copolymer was eliminated faster than the hyperbranched dendrimer, even though it was slightly greater in hydrodynamic size. However, for the higher molecular weight polymers, G7.0-OH has a faster clearance than the HPMA copolymer (131 kDa) of comparable MW. In this range of MW, the G7.0-OH was almost half the hydrodynamic size of HPMA (131 kDa) and the vast difference in hydrodynamic size governed the elimination clearance.

Over the molecular weight range studied, elimination clearance decreased log linearly with increase in hydrodynamic size within each of the polymer series (Figure 4). However, elimination clearance decreased more rapidly for PAMAM-OH dendrimers with increase in hydrodynamic volume as compared to HPMA copolymers indicated by slopes (Figure 4). This can be attributed to the effect of architecture on the change in molecular conformation of polymers with increase in molecular weight (elaborated in detail in the Discussion Section) [20, 21].

The observed trend of decrease in elimination clearance is only expected to hold over this range of molecular weights since the polymers transition from being small enough to be readily filtered through the kidney (G5.0-OH and HPMA copolymer (26 kDa)), to being on the threshold of kidney filtration (G6.0-OH, HPMA copolymer (52 kDa)), and further to being long circulating in the plasma (G7.0-OH, HPMA copolymer (131 kDa)) with a minimal renal clearance. We do not expect this trend to hold outside of this molecular weight or size range, where the elimination clearance is likely to be independent of hydrodynamic size, although such studies warrant further investigation [22].

3.2.3. Renal Clearance—Renal clearance decreased with increase in hydrodynamic size for each of the polymer series (Table 2, Figure 5). However, at comparable molecular weights, linear HPMA copolymers were eliminated renally to a higher extent (by an order of magnitude) than hyperbranched PAMAM-OH dendrimers (Table II, Figure 5). In spite of the hydrodynamic size of HPMA copolymer (131 kDa) (R_h = 8.2 nm) being double that of G7.0-OH (R_h = 4.0 nm), HPMA copolymer (131 kDa) was eliminated renally to a greater extent than G7.0-OH. This can be attributed to the unique ability of a linear polymer to reptate through a renal filtration pore while the branched polymer has to deform in order to pass through [15, 23]. Renal clearance was significantly less than the total elimination clearance for all of the polymers under study. This is indicative of the presence of other clearance mechanisms, potentially through the liver and the spleen.

3.2.4. Tumor exposure—Tumor concentration peaked at about 0.5–6 hours for the polymers under study with the larger molecular weight polymers showing a greater T_{max} than the lower molecular weight polymers (Figure 6A) indicating a longer diffusion time for the larger polymers into the tumor. The dose normalized tumor exposure (AUC_{tumor}/dose) increased with increase in molecular weight or hydrodynamic size within a given polymer series (Table 2, Figure 6B). However, the tumor exposure of the PAMAM-OH dendrimers was greater than that of HPMA copolymers of comparable molecular weights. In spite of a

smaller hydrodynamic radius, faster elimination and lesser plasma exposure, G7.0-OH (Rh = 4.0 nm) accumulated in the tumor twice as much as HPMA copolymer (131 kDa) (Rh = 8.2 nm) of comparable MW. The tumor to plasma exposure ratios indicate that the polymers in circulation passively accumulated in the tumor and this accumulation was greater for the PAMAM dendrimers than the HPMA copolymers under study. The tumor to plasma exposure ratios suggest that when in circulation, PAMAM-OH dendrimers have a higher affinity to accumulate in the tumor than the HPMA copolymers (Figure 7).

3.2.5 Plasma and Tumor extravasation and elimination rate constants—In accordance with the trend in elimination clearance, discussed in detail in Section 3.2.2, plasma elimination rate constant (K_1) generally decreased with increase in molecular weight/hydrodynamic size of polymers within a given series (Table III). As a consequence of increased plasma circulation, tumor extravasation rate constant (K_2) increased with increase in molecular weight/hydrodynamic size within a polymer series (Table III). Amongst the lower molecular weight polymers, G5.0-OH and G6.0-OH extravasated into the tumor faster than their equivalent molecular weight counterparts in the HPMA copolymer series. For the higher molecular weight pomyers-G7.0-OH and HPMA copolymer (131 kDa), tumor extravasation rates were comparable.

In agreement with the EPR effect, rate constant K_6 which facilitated prolonged tumor retention of the polymers over the time period of study increased with increase in molecular weight of polymers within a given series (Table III). Across polymers of different architecture, the PAMAM dendrimers had K_6 values an order of magnitude higher than the HPMA copolymers of comparable molecular weight. This suggests that PAMAM dendrimers had higher tumor retention than HPMA copolymers in the orthotopic xenograft ovarian tumors under study. This propensity of the PAMAM dendrimers to passively target the tumor was also reflected in tumor to plasma exposure ratios of the polymer discussed in Section 3.2.4.

4. DISCUSSION

Polymeric carriers used in drug delivery have a favorable pharmacokinetic profile over small molecular weight drugs owing to their reduced renal clearance and resulting long circulation half-life in the blood [24]. Unlike small molecular weight drugs which are known to have instantaneous distribution into blood-perfused organs, macromolecular distribution to both target organs such as tumor, and clearance organs such as kidney and liver is limited by their size [24]. Target organs like the tumor are known to have increased uptake and retention of macromolecules due to the enhanced permeability and retention effect [25]. The extent of accumulation of macromolecules in these organs and their blood pharmacokinetics depend on their physicochemical attributes such as chemical composition, molecular weight, hydrodynamic size, charge, extent of plasma protein binding and molecular architecture [26]. Architecture of a polymeric carrier is determined by its molecular conformation, chain flexibility, deforming capability and extent of branching [15]. The polymeric carriers that were evaluated had distinct architectures: PAMAM-OH dendrimers which are hyperbranched polymers with a globular shape while the HPMA copolymers which are linear polymers with side chains known to assume a random coil conformation in solution [20, 21]. PAMAM dendrimers become more rigid at higher generations [5, 20]. With every increase in generation, extent of branching increases and so does surface congestion. This affects the molecular conformation and deforming capability of the dendrimer. The smaller generation PAMAMs (G0.0-3.0) are flexible, floppy and disc-like. Generations 4.0 through 6.0 have a hollow core and permeable outer shells that render them as nano-containers. Generations 7.0 onwards, the dendrimers start to possess a very rigid surface scaffolding with a globular shape [5]. The PAMAM-OH dendrimers under study, i.e., G5.0 through

G7.0 lie in a range where they transition from a more flexible conformation for G5.0-OH to a more rigid, globular shape for G7.0-OH. The HPMA copolymers on the other hand are not known to undergo a significant conformational change for the range of molecular weights that were studied (26–131 kDa). This trend in molecular conformational change of polymers of different architecture affected their pharmacokinetics. The polymers under study interacted minimally with plasma proteins due to their neutral charge (Section V, online resource). Hence, we do not expect plasma protein binding to influence observed trends in biodistribution and pharmacokinetics.

Elimination clearance decreased more rapidly for PAMAM dendrimers with increase in molecular weight or hydrodynamic size than for HPMA copolymers for the same increase in molecular weight (Figure 3). These results are in agreement with other studies which show that the shape and ability of the polymer to deform play important roles in the glomerular filtration rate and hence elimination clearance [15, 16, 27, 28]. Previous reports suggest that increased hydrodynamic size, decreased flexibility and increased extent of branching of polymer chains limits passage of a polymer through a pore of comparable size and reduces elimination through the kidneys [15]. *In vitro* diffusion studies of polymers through porous structures have shown that transport of linear polymers in tissue containing complex extracellular matrix is different from that of branched polymers [23, 29–32]. The exponent for power law stating the molecular weight dependence on diffusion coefficient through a membrane with defined pore sizes is different for a linear (exponent = −1 to −2.5) versus branched (exponent = −0.33) polymer. These observations are explained by de Gennes's polymer reptation theory where a linear polymer can move through a network of fibrous obstacles presented by the extracellular matrix while the branched polymer cannot [33]. The branched polymer has to deform in order to diffuse through. *In vivo*, the glomerular basement membrane, which is a complex fibrous network is known to be the primary barrier to filtration of neutral macromolecules [34]. Hence, it has been considered fairly realistic to apply the theory of molecular sieving in polymeric gels to the glomerular filtration of macromolecules [34]. For the lower molecular weight polymers, in spite of a higher hydrodynamic radius, G5.0-OH (R_h = 2.3 nm) eliminated faster than HPMA copolymer (26 kDa) (R_h = 1.4 nm), possibly due to a compact and flexible structure that allowed faster extravasation. The conformational change of PAMAM dendrimers with increase in hydrodynamic size can affect their deforming capability and drastically reduce transport through the capillary endothelium of clearance organs thereby reducing their clearance. G6.0-OH (R_h = 3.0 nm) eliminated slower than HPMA copolymer (52 kDa) (R_h = 3.3 nm) of comparable MW, possibly due to increased rigidity and consequently slower extravasation. HPMA copolymers, owing to a linear architecture can potentially reptate through pores of capillary endothelium, even if their effective hydrodynamic radii are greater than pore size of fenestration. Hence, even though the elimination clearance for G7.0-OH (R_h = 4.0 nm) was greater than HPMA copolymer (131 kDa) (R_h = 8.2 nm) of comparable MW, the rate at which the elimination clearance changed over a fixed MW range was different for the two polymers of varying architecture. The elimination clearance changed less rapidly with increase in molecular weight and hydrodynamic size of HPMA copolymers as compared to PAMAM dendrimers. In addition to differences in interstitial transport rates of PAMAM-OH dendrimers and HPMA copolymers, their intrinsic differences in physicochemical properties could potentially alter their rate and extent of endocytosis and transcytosis through cells, directly affecting their plasma clearances. Extensive kidney accumulation of G5.0-OH and liver accumulation of G6.0-OH also suggests differences in cellular uptake of these polymers based on size and architecture [17].

Renal clearance showed a trend similar to the elimination clearance where along with hydrodynamic size, the polymer architecture affected this parameter (Figure 5). The effective pore size for glomerular filtration through the kidney is 3.7–6.0 nm in

hydrodynamic diameter [19]. PAMAM G5.0-OH and HPMA copolymer (26 kDa) fall below the size cutoff of glomerular filtration and should readily eliminate through the kidneys. However, renal clearance of G5.0-OH was less than HPMA copolymers of comparable molecular weight since G5.0-OH showed persistent accumulation in the kidney (upto 80% injected dose) [17]. Limited mechanistic studies for renal retention of PAMAM dendrimers report the localization of these polymers in the lysosomes of proximal tubule cells upon glomerular filtration of the dendrimers [35]. G6.0-OH (R_h = 3.0 nm) and HPMA copolymer (52 kDa) (R_h = 3.3 nm) are comparable in hydrodynamic size and fall on the threshold of the size cutoff range for kidney filtration. HPMA copolymer (52kDa) was renally cleared to a higher extent than G6.0-OH. HPMA copolymer (131 kDa) (R_h = 8.2 nm) is twice the hydrodynamic size of G7.0-OH (R_h = 4.0 nm), and yet was renally cleared to a greater extent than its PAMAM counterpart of comparable MW. This can be explained by the architectural difference in the two constructs. The primary impediment to renal clearance of these polymers is likely to be the tortuous path though the fibrous mesh of the glomerular basement membrane [34]. While the linear HPMA copolymers can potentially reptate through a pore smaller in size than their hydrodynamic radii in a random coil conformation, PAMAM dendrimers have to deform in order to permeate across the pores (Figure 8). With increase in molecular weight or generation, the deforming capacity of PAMAM-OH dendrimers is known to decrease, making it harder for higher generation PAMAM-OH dendrimers to sieve through the glomerulus as compared to HPMA copolymers of comparable molecular weights.

Renal clearance was however significantly less than the total elimination clearance suggesting clearance through the liver and spleen. It could also suggest distribution of the polymers into other compartments outside the central compartment (plasma). Specifically renal clearance was significantly less for PAMAM dendrimers than HPMA polymers. PAMAM-OH dendrimers showed high liver accumulation (15–50% injected dose/g of liver tissue), which could potentially facilitate biliary clearance [17].

Polymer concentration in a given tumor type is a function of plasma clearance rate and vascular exposure along with kinetics of transendothelial transport within the tumor or effective interstitial diffusion coefficient [36, 26]. These factors are governed by a number of physicochemical characteristics of the polymer including size, surface characteristics, shape, and rigidity [26]. Of these properties affecting interstitial tumor transport, the molecular conformation or polymer architecture has been the least studied. In general, polymers with a flexible conformation have demonstrated more ideal tumor transport properties leading to higher tumor accumulation [37–39]. Findings reported in this paper however are contradicting this trend with the globular, rigid PAMAM dendrimers showing higher tumor to plasma exposure ratio and extravsation rate constants (K_2, K_6) than the random coil, flexible HPMA copolymers of comparable MW (Figure 7). This could be indicative of a phenomenon in the complex fibrous extracellular matrix of angiogenic neovasculature where rigid nanoscale constructs may show higher permeability than coiled polymers that can entangle in the matrix. Besides the conformation, the difference in hydrodynamic size of polymers of varying architecture and comparable molecular weights could also contribute to differences in tumor extravsation rate constant (K_6) and total exposure (AUC_{tumor}/dose). For instance, HPMA copolymer (131 kDa) (R_h = 8.2 nm) is twice the hydrodynamic size of G7.0-OH (R_h = 4.0 nm) of comparable molecular weight. It is known that the primary impediment for the transvascular extravasation of particles across the blood-tumor-barrier is at the level of the glycocalyx that coats the surface of pores formed in the trans-endothelial cell fenestrations and inter-endothelial cell gaps [26, 29]. The luminal glycocalyx layer acts as a nanofilter for transvascular flow creating an effective physiological upper limit of pore size for the blood-tumor-barrier [26, 29]. This pore size cutoff can vary for different tumor types and is not precisely known for the orthotopic

xenograft A2780 ovarian carcinoma tumors under study. However, based on the pore size range for other tumor types, it could range between the hydrodynamic sizes of HPMA copolymer (131 kDa) and G7.0-OH [40]. This could potentially explain the difference in tumor accumulation of these higher molecular weight polymers. These findings suggest that further investigation and optimization of polymer size and conformation is necessary for optimal tumor transport/accumulation.

5. CONCLUSION

Along with molecular weight and hydrodynamic size, polymer architecture was critical in affecting the blood pharmacokinetics of the PAMAM-OH dendrimers and HPMA copolymers. Over the molecular weight range studied, elimination clearance decreased more rapidly with increase in R_h for PAMAM-OH dendrimers as compared to HPMA copolymers. Linear HPMA copolymers were eliminated renally to a higher extent than hyperbranched PAMAM-OH dendrimers. These results were indicative of a difference in extravasation of polymers of varying architecture through fenestrations of the kidney tissue. In addition, PAMAM-OH dendrimers had a higher tumor to plasma exposure ratio than HPMA copolymers indicating that when in circulation, PAMAM-OH were taken up in the tumor to a greater extent than HPMA copolymers suggesting that polymer architecture influenced tumor extravasation and retention.

Supplementary Material

Refer to Web version on PubMed Central for supplementary material.

Acknowledgments

The authors acknowledge Nate Larson for providing monomers for and guidance with HPMA copolymer synthesis. The authors also acknowledge Yong En Sun for assistance with tumor inoculations and organ harvesting. Financial support was provided by the National Library of Medicine (NLM) Bethesda, Maryland Grant # 5 T15 LM 7124 and by National Institute of Health (NIH) grants R01 R01DE019050 and R01EB07470, the Utah Science Technology and Research (USTAR) initiative and a University of Utah Graduate Research Fellowship.

Abbreviations

PAMAM	poly(amido amine)
PAMAM-OH	hydroxyl terminated poly(amido amine)
HPMA	*N*-(2-hydroxypropyl)methacrylamide
GX.0-OH	hydroxyl terminated PAMAM, generation X.0
R_h	hydrodynamic radius
MW	molecular weight
C_p	concentration in the plasma
C_{t1}	concentration in tumor compartment 1
C_{t2}	concentration in tumor compartment 2
AUC_{plasma}	area under the curve of the plasma concentration profile
AUC_{tumor}	area under the curve of the tumor concentration profile
E.CL	elimination clearance
CL_R	renal clearance

AIC	Akaike information criterion

References

1. Duncan R. The dawning era of polymer therapeutics. Nat Rev Drug Discovery. 2003; 2(5):347–60.
2. Qiu LY, Bae YH. Polymer architecture and drug delivery. Pharm Res. 2006; 23(1):1–30. [PubMed: 16392022]
3. Esfand R, Tomalia DA. Poly (amidoamine)(PAMAM) dendrimers: from biomimicry to drug delivery and biomedical applications. Drug Discovery Today. 2001; 6(8):427–36. [PubMed: 11301287]
4. Tomalia DA, Baker H, Dewald J, Hall M, Kallos G, Martin S, et al. A new class of polymers: starburst-dendritic macromolecules. Polym J. 1985; 17(1):117–32.
5. Tomalia D, Reyna L, Svenson S. Dendrimers as multi-purpose nanodevices for oncology drug delivery and diagnostic imaging. Biochem Soc Trans. 2007; 35:61–7. [PubMed: 17233602]
6. Duncan R, Izzo L. Dendrimer biocompatibility and toxicity. Adv Drug Deliv Rev. 2005; 57(15): 2215–37. [PubMed: 16297497]
7. Malik N, Wiwattanapatapee R, Klopsch R, Lorenz K, Frey H, Weener JW, et al. Dendrimers: relationship between structure and biocompatibility *in vitro*, and preliminary studies on the biodistribution of 125I-labelled polyamidoamine dendrimers *in vivo*. J Control Release. 2000; 65(1–2):133–48. [PubMed: 10699277]
8. Wijagkanalan W, Kawakami S, Hashida M. Designing dendrimers for drug delivery and imaging: pharmacokinetic considerations. Pharm Res. 2011; 28(7):1500–19. [PubMed: 21181549]
9. Duncan R. Development of HPMA copolymer-anticancer conjugates: clinical experience and lessons learnt. Adv Drug Deliv Rev. 2009; 61(13):1131–48. [PubMed: 19699249]
10. Kopecek J, Kopecková P. HPMA copolymers: origins, early developments, present, and future. Adv Drug Deliv Rev. 2010; 62(2):122–49. [PubMed: 19919846]
11. Borgman M, Coleman T, Kolhatkar R, Geyser-Stoops S, Line B, Ghandehari H. Tumor-targeted HPMA copolymer-(RGDfK)-(CHX-A″-DTPA) conjugates show increased kidney accumulation. J Controlled Release. 2008; 132(3):193–9.
12. Konak C, Rathi RC, Kopeckova P, Kopecek J. Effect of side-chains on solution properties of N-(2-hydroxypropyl) methacrylamide copolymers in aqueous solvents. Polymer. 1993; 34(22):4767–73.
13. Lammers T, Kuhnlein R, Kissel M, Subr V, Etrych T, Pola R, et al. Effect of physicochemical modification on the biodistribution and tumor accumulation of HPMA copolymers. J Control Release. 2005; 110(1):103–18. [PubMed: 16274831]
14. Chen B, Jerger K, Fréchet JMJ, Szoka FC Jr. The influence of polymer topology on pharmacokinetics: Differences between cyclic and linear PEGylated poly (acrylic acid) comb polymers. J Control Release. 2009; 140(3):203–9. [PubMed: 19465070]
15. Fox ME, Szoka FC, Fre chet JMJ. Soluble polymer carriers for the treatment of cancer: the importance of molecular architecture. Accounts Chemical Res. 2009; 42(8):1141–51.
16. Nasongkla N, Chen B, Macaraeg N, Fox ME, Fre chet JMJ, Szoka FC. Dependence of pharmacokinetics and biodistribution on polymer architecture: effect of cyclic versus linear polymers. J Am Chem Soc. 2009; 131(11):3842–3. [PubMed: 19256497]
17. Sadekar S, Ray A, Jana t-Amsbury M, Peterson C, Ghandehari H. Comparative biodistribution of PAMAM dendrimers and HPMA copolymers in ovarian-tumor-bearing mice. Biomacromolecules. 2011; 12(1):88–96. [PubMed: 21128624]
18. Cutnell, JJ.; Kenneth. Physics. 4. Wiley; 1998.
19. Rippe C, Asgeirsson D, Venturoli D, Rippe A, Rippe B. Effects of glomerular filtration rate on Ficoll sieving coefficients (theta) in rats. Kidney Int. 2006; 69(8):1326–32. [PubMed: 16395274]
20. Tande B, Wagner N, Mackay M, Hawker C, Jeong M. Viscosimetric, hydrodynamic, and conformational properties of dendrimers and dendrons. Macromolecules. 2001; 34(24):8580–5.
21. Ulbrich K, Subr V. Structural and chemical aspects of HPMA copolymers as drug carriers. Adv Drug Deliv Rev. 2010; 62(2):150–66. [PubMed: 19931329]

22. Schmidt MM, Wittrup KD. A modeling analysis of the effects of molecular size and binding affinity on tumor targeting. Mol Cancer Ther. 2009; 8(10):2861–71. [PubMed: 19825804]
23. Deen W, Bohrer M, Epstein N. Effects of molecular size and configuration on diffusion in microporous membranes. AIChE Journal. 1981; 27(6):952–9.
24. Nishikawa M, Takakura Y, Hashida M. Pharmacokinetic evaluation of polymeric carriers. Adv Drug Deliv Rev. 1996; 21(2):135–55.
25. Maeda H, Wu J, Sawa T, Matsumura Y, Hori K. Tumor vascular permeability and the EPR effect in macromolecular therapeutics: a review. J Control Release. 2000; 65(1–2):271–84. [PubMed: 10699287]
26. Chauhan VP, Stylianopoulos T, Boucher Y, Jain RK. Delivery of molecular and nanoscale medicine to tumors: Transport barriers and strategies. Annu Rev Chem Biomol. 2011; 2:281–98.
27. Gillies ER, Dy E, Fréchet JMJ, Szoka FC. Biological evaluation of polyester dendrimer: poly (ethylene oxide)"bow-tie" hybrids with tunable molecular weight and architecture. Mol Pharm. 2005; 2(2):129–38. [PubMed: 15804187]
28. Lim J, Guo Y, Rostollan CL, Stanfield J, Hsieh JT, Sun X, et al. The role of the size and number of polyethylene glycol chains in the biodistribution and tumor localization of triazine dendrimers. Mol Pharm. 2008; 5(4):540–7. [PubMed: 18672950]
29. Jain RK. Transport of molecules in the tumor interstitium: a review. Cancer Res. 1987; 47(12): 3039. [PubMed: 3555767]
30. Ohlson M, Sörensson J, Lindström K, Blom AM, Fries E, Haraldsson B. Effects of filtration rate on the glomerular barrier and clearance of four differently shaped molecules. Am J Physiol-Renal. 2001; 281(1):F103.
31. Venturoli D, Rippe B. Ficoll and dextran vs. globular proteins as probes for testing glomerular permselectivity: effects of molecular size, shape, charge, and deformability. Am J Physiol-Renal. 2005; 288(4):F605.
32. Pluen A, Netti PA, Jain RK, Berk DA. Diffusion of macromolecules in agarose gels: comparison of linear and globular configurations. Biophys J. 1999; 77(1):542–52. [PubMed: 10388779]
33. Gennes, PGd. Reptation of a polymer chain in the presence of fixed obstracles. J Chem Phys. 1971; 55(2):572–9.
34. Deen WM, Bohrer MP, Brenner BM. Macromolecule transport across glomerular capillaries: application of pore theory. Kidney Int. 1979; 16(3):353–65. [PubMed: 529682]
35. Kobayashi H, Kawamoto S, Jo SK, Sato N, Saga T, Hiraga A, et al. Renal tubular damage detected by dynamic micro-MRI with a dendrimer-based magnetic resonance contrast agent. Kidney Int. 2002; 61(6):1980–5. [PubMed: 12028438]
36. Dreher MR, Liu W, Michelich CR, Dewhirst MW, Yuan F, Chilkoti A. Tumor vascular permeability, accumulation, and penetration of macromolecular drug carriers. J Natl Cancer Inst. 2006; 98(5):335–44. [PubMed: 16507830]
37. Uzgiris E. The role of molecular conformation on tumor uptake of polymeric contrast agents. Invest Radiol. 2004; 39(3):131–7. [PubMed: 15076004]
38. Uzgiris E, Cline H, Moasser B, Grimmond B, Amaratunga M, Smith JF, et al. Conformation and structure of polymeric contrast agents for medical imaging. Biomacromolecules. 2004; 5(1):54–61. [PubMed: 14715008]
39. Uzgiris E. A Cell-Surface Polymer Reptation Mechanism for Tumor Transendothelial Transport of Macromolecules. Technol Cancer Res T. 2008; 7(3):257–68.
40. Sarin H, Kanevsky AS, Wu H, Sousa AA, Wilson CM, Aronova MA, et al. Physiologic upper limit of pore size in the blood-tumor barrier of malignant solid tumors. J Transl Med. 2009; 7(1):51. [PubMed: 19549317]

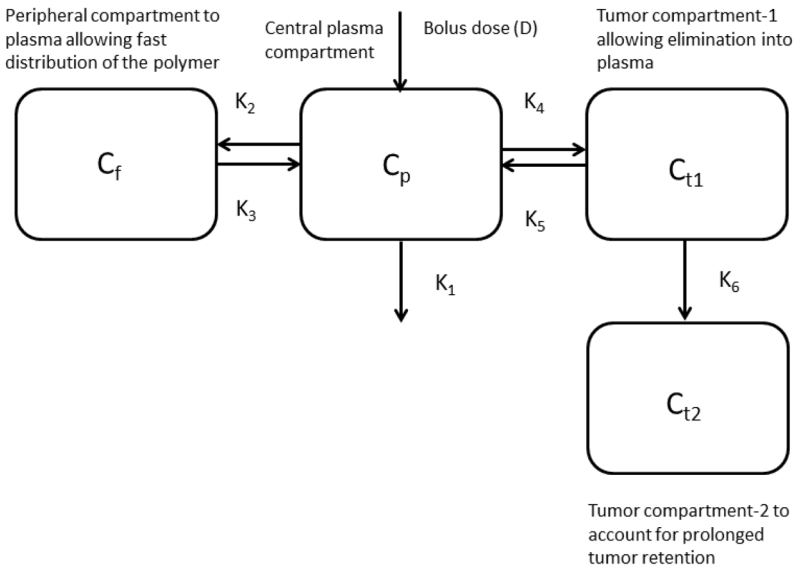

Figure 1.
Compartmental model linking the plasma and the tumor compartment.

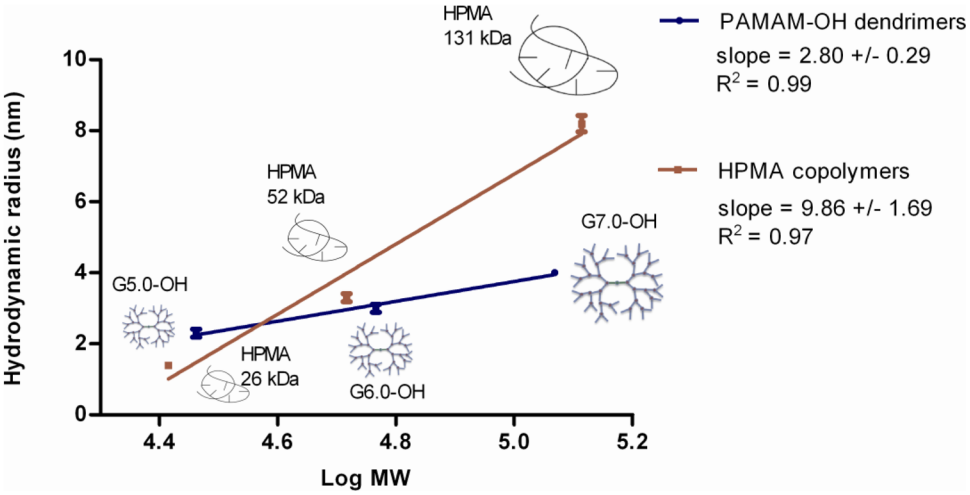

Figure 2.
Correlation of hydrodynamic radii to molecular weights of PAMAM dendrimers and HPMA copolymers. Data is represented as mean ± S.D, n=3. Reprinted (Adapted) with permission from [17], Copyright (2011) American Chemical Society.

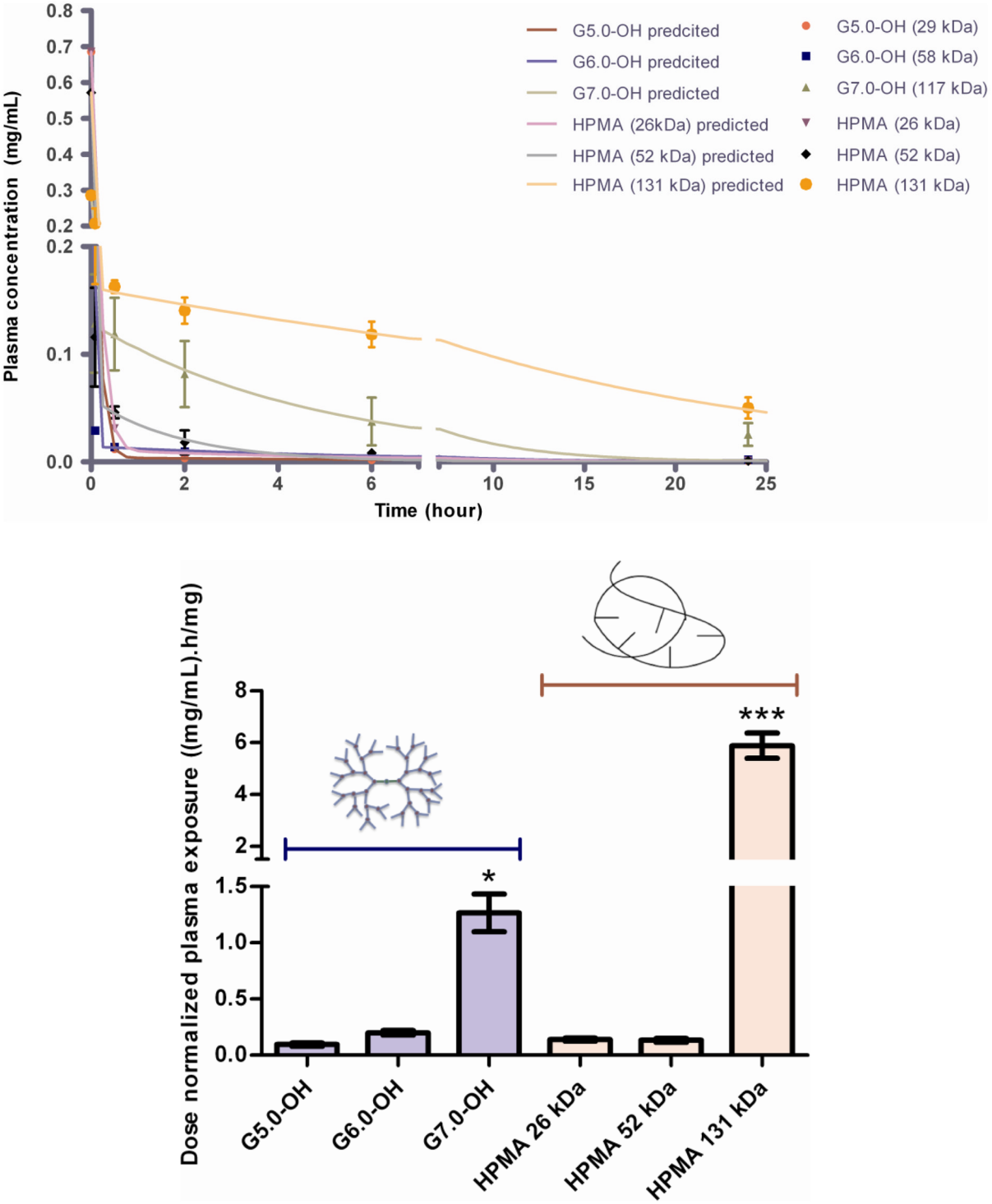

Figure 3.

A. Plasma concentration profile of PAMAM-OH dendrimers and HPMA copolymers with time. Experimental data is represented in symbols-mean ± SEM. Model predicted best fit values are represented as a line. Reprinted (Adapted) with permission from [17], Copyright (2011) American Chemical Society. **B.** Dose normalized plasma exposure (0–24 h) of

PAMAM-OH dendrimers and HPMA copolymers. Data is represented as mean estimate ± standard error of fit. Dose normalized plasma exposure of G7.0-OH and HPMA 131 kDa is statistically significantly different from lower MW polymers with $p<0.5$ and $p<0.001$ respectively.

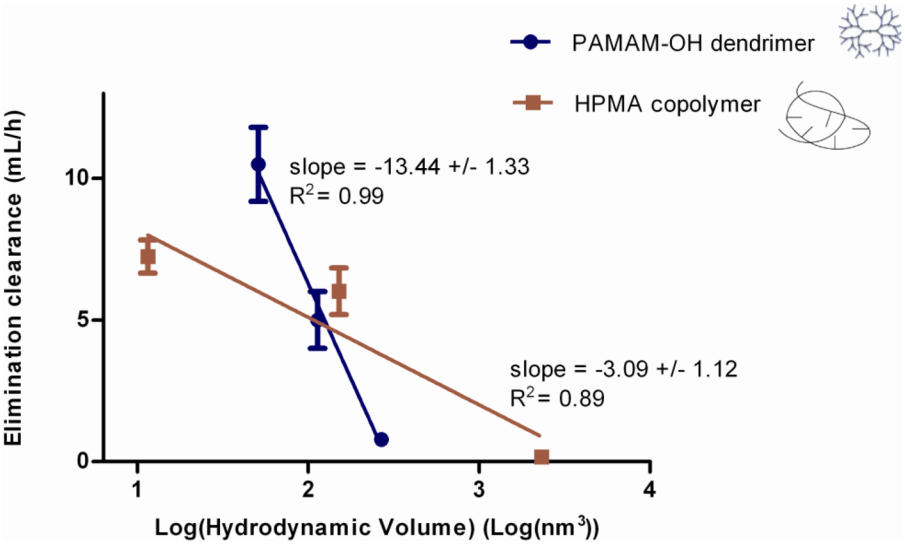

Figure 4.
Correlation of elimination clearance of PAMAM-OH dendrimers and HPMA copolymers to hydrodynamic size. Data is represented as mean estimate ± standard error of fit.

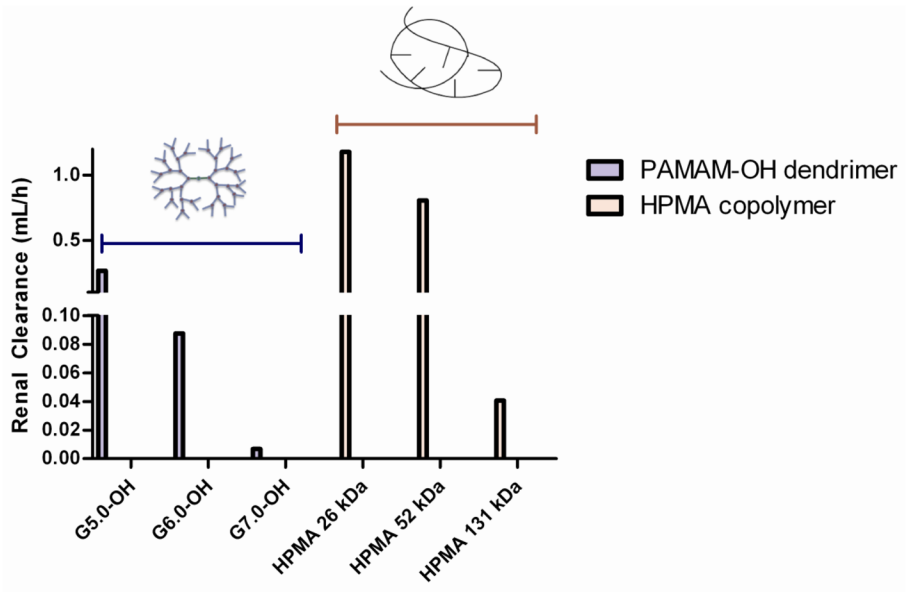

Figure 5.

Renal clearances of PAMAM-OH dendrimers and HPMA copolymers. Data is represented as mean clearance calculated from data pooled for all animals in each treatment group.

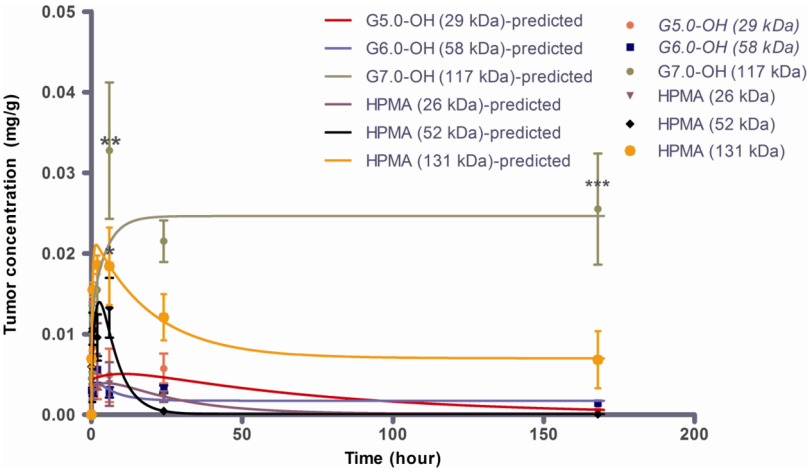

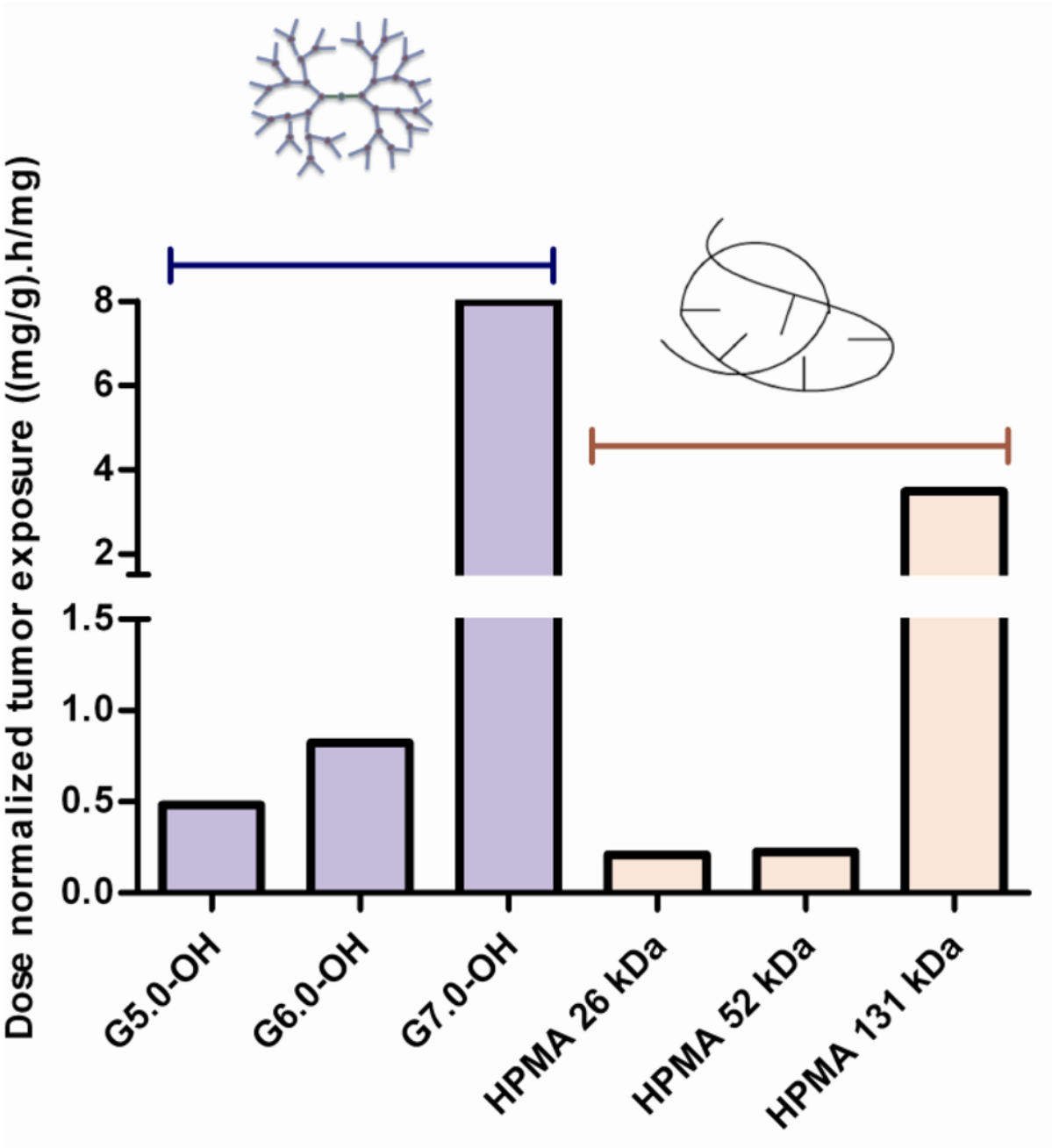

Figure 6.

A. Tumor concentration profile of PAMAM-OH dendrimers and HPMA copolymers with time. Experimental data is represented in symbols-mean ± SEM. Model predicted best fit values are represented as a line. Tumor accumulation of G7.0-OH is statistically significantly higher than HPMA 131 kDa at 6 hours and 24 hours with a $p<0.01$ and $p<0.001$ respectively; Tumor accumulation of HPMA 131 KDa is higher than accumulation of lower MW polymers (except G7.0-OH) at 6 hours, $p<0.5$. Reprinted (Adapted) with permission from [17], Copyright (2011) American Chemical Society. **B.** Dose normalized tumor exposure (0–168 h) of PAMAM-OH dendrimers and HPMA copolymers. Mean exposure values are computed from area under the curve of the tumor concentration profile.

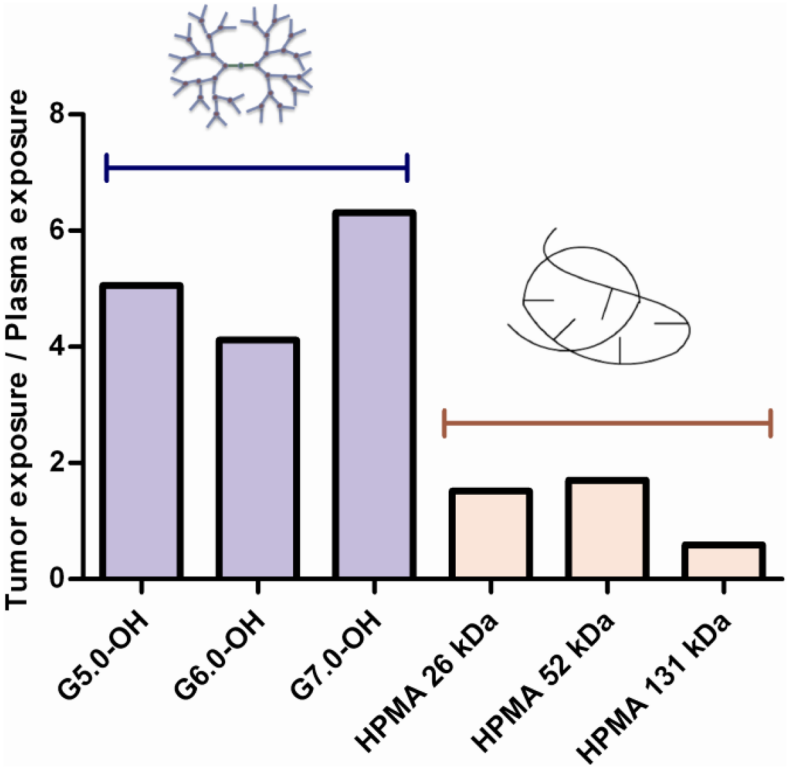

Figure 7.
Ratio of tumor/plasma exposure of PAMAM-OH dendrimers and HPMA copolymers.

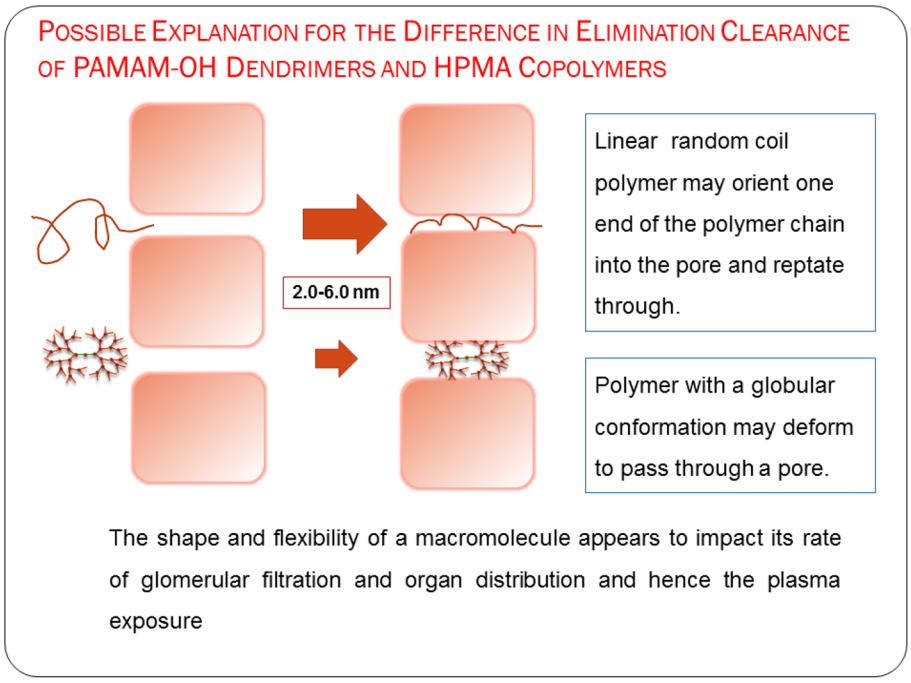

Figure 8.
Proposed explanation for the difference in elimination clearance of PAMAM-OH dendrimers and HPMA copolymers, Adapted from Ref [15].

Table I

Physicochemical Characteristics of PAMAM dendrimers and HPMA copolymers. Reprinted (Adapted) with permission from [17], Copyright (2011) American Chemical Society.

Polymer	G5.0-OH	G6.0-OH	G7.0-OH	HPMA copolymers		
Weight average molecular weight (kDa)	28.950 *	58.298 *	116.993 *	26.0 ± 2.0	52.0 ± 5.0	131.0 ± 0.3
Poly dispersity Index	ND	ND	ND	1.3 ± 0.2	1.9 ± 0.2	1.7 ± 0.1
Hydrodynamic radius (R_h) (nm)	2.3 ± 0.2	3.0 ± 0.2	4.0 ± 0.1	1.4 ± 0.0	3.3 ± 0.2	8.2 ± 0.4
Zeta Potential (mV)	1.69 ± 0.21	2.28 ± 0.48	−1.3 ± 0.06	−14.66 ± 0.83	−1.46 ± 0.29	−19.2 ± 1.4
Number of surface hydroxyl groups	128 *	256 *	512 *	ND	ND	ND

* Theoretical values based on perfect dendrimer synthesis [4]; Values are Mean +/− SD (n=3).

Values for all polymers are from Ref [17] except HPMA copolymer (131 KDa) which was sythesized for this study.

Table II

Plasma compartmental pharmacokinetic parameter estimates for PAMAM-OH dendrimers and HPMA copolymers.

Parameter	G5.0-OH (29 kDa)	G6.0-OH (58 kDa)	G7.0-OH (117 kDa)	HPMA copolymer (26 kDa)	HPMA copolymer (52 kDa)	HPMA copolymer (131 kDa)
Clearance (mL/h)						
Elimination Clearance (E.CL)	10.50 ± 1.30	5.00 ± 1.00	0.79 ± 0.21	7.24 ± 0.58	6.02 ± 0.82	0.17 ± 0.03
Renal Clearance (CL_R)	0.266	0.087	0.007	1.179	0.807	0.041
Dose normalized Exposure						
$AUC_{plasma(0–24h)}$ (mg.h/mg.mL)	0.1 ± 0.01	0.2 ± 0.04	1.27 ± 0.34	0.14 ± 0.01	0.13 ± 0.02	5.88 ± 0.97
$AUC_{tumor(0–168h)}$ (mg.h/mg.g)	0.48	0.82	7.99	0.21	0.23	3.48
AUC_{tumor}/AUC_{plasma}	5.06	4.12	6.31	1.52	1.70	0.59

Elimination clearance and plasma exposure were computed by two-compartmental analysis with bolus input. Renal clearances were computed from urine data. Tumor AUCs were computed from area under the tumor concentration profile curve. Data is presented as mean ± standard error.

Table III

Extravasation and elimination rate constants of the plasma-tumor link model.

Parameter (h^{-1})	G5.0-OH (29 kDa)	G6.0-OH (58 kDa)	G7.0-OH (117 kDa)	HPMA copolymer (26 kDa)	HPMA copolymer (52 kDa)	HPMA copolymer (131 kDa)
K_1	6.000	2.860	0.451	4.137	4.300	0.097
K_2	2.807	30.168	27.460	2.702	18.886	4.953
K_3	0.161	1.877	22.817	0.275	3.088	6.301
K_4	0.056	0.312	0.381	0.035	0.193	0.358
K_5	0.014	0.915	3.213	0.045	0.196	2.334
K_6	0.000	0.054	0.405	0.001	0.001	0.016

K_1, K_2 and K_3 were determined from two-compartmental modeling of plasma concentration data using Winnonlin®.

K_4, K_5 and K_6 were determined from plasma-tumor link model fitted to experimental plasma and tumor data using a multivariable constrained optimization solver in Matlab®.